Journal of Sound and Vibration (2000) **231**(4), 1159–1167
Article No. jsvi.1999.2467, available online at http://www.idealibrary.com on IDEAL®

LETTERS TO THE EDITOR

ACOUSTIC ATTENUATION PERFORMANCE OF EXPANSION CHAMBERS WITH TWO END-INLETS/ONE SIDE-OUTLET

A. Selamet and Z. L. Ji

Department of Mechanical Engineering and The Center for Automotive Research, The Ohio State University, Columbus, OH 43210-1107, U.S.A.

(*Received* 11 *June* 1999)

1. INTRODUCTION

The expansion chamber with single inlet/outlet is a common silencer in pulsating internal flows, and has been investigated extensively [1–12]. The studies demonstrated that the expansion chambers with end-inlet and end-outlet exhibit the attenuation dome behaviour, while the expansion chambers with side-inlet and/or side-outlet reveal the combination of the attenuation domes and the resonance peaks below the cut-off frequency of the first excited order mode of the chamber.

The expansion chamber with two inlets and one outlet is another practical and important configuration which may be used in the exhaust system of reciprocating engines to merge two gas streams into one common tailpipe. It appears, however, the acoustic attenuation performance of this configuration has not been investigated thus far in the literature. The present study considers a circular expansion chamber with two end-inlets and one side-outlet. The objective is then (1) to present a simple one-dimensional approach to estimate the transmission loss of the chamber; (2) to apply the boundary element method (BEM) to predict acoustic attenuation of the chamber and to assess the accuracy and applicability of the 1-D solutions; and (3) to investigate the effects of geometry and incident wave conditions on the acoustic attenuation performance of the chamber.

2. ONE-DIMENSIONAL APPROACH

Consider the expansion chambers with two end-inlets and one side-outlet shown in Figure 1. Assuming plane wave propagation in the axial direction, the continuity conditions of the acoustic pressure and volume velocity give
at the inlet 1:

$$p_1^+ + p_1^- = p_4^+ + p_4^-, \tag{1}$$

$$p_1^+ - p_1^- = m_1(p_4^+ - p_4^-), \tag{2}$$

at the inlet 2:

0022-460X/00/141159 + 09 $35.00/0

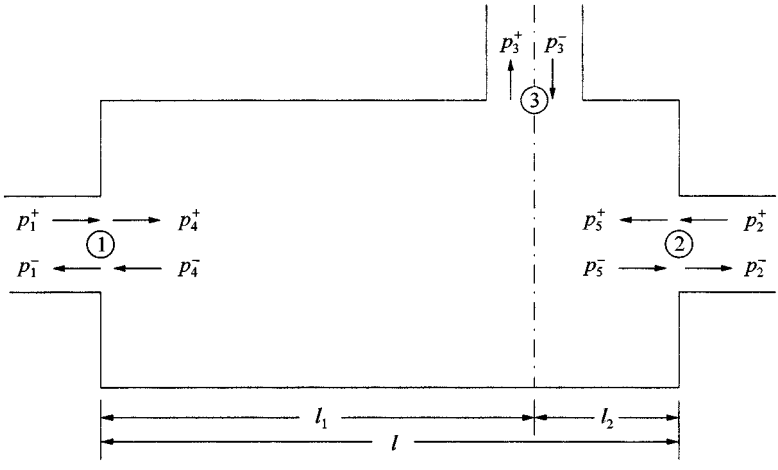

Figure 1. An expansion chamber with two end-inlets/one side-outlet.

$$p_2^+ + p_2^- = p_5^+ + p_5^-, \tag{3}$$

$$p_2^+ - p_2^- = m_2(p_5^+ - p_5^-), \tag{4}$$

and at the outlet 3:

$$p_4^+ \mathrm{e}^{-\mathrm{j}kl_1} + p_4^- \mathrm{e}^{\mathrm{j}kl_1} = p_3^+ + p_3^-, \tag{5}$$

$$p_5^+ \mathrm{e}^{-\mathrm{j}kl_2} + p_5^- \mathrm{e}^{\mathrm{j}kl_2} = p_3^+ + p_3^-, \tag{6}$$

$$p_4^+ \mathrm{e}^{-\mathrm{j}kl_1} - p_4^- \mathrm{e}^{\mathrm{j}kl_1} + p_5^+ \mathrm{e}^{-\mathrm{j}kl_2} - p_5^- \mathrm{e}^{\mathrm{j}kl_2} = (p_3^+ - p_3^-)/m_3, \tag{7}$$

where $m_1 = S/S_1, m_2 = S/S_2, m_3 = S/S_3$, and S, S_1, S_2 and S_3 are the cross-sectional areas of chamber, two-inlet and outlet ducts, respectively; the superscript + and − denote the incident and reflected waves.

For the non-reflecting outlet case ($p_3^- = 0$), equations (1)–(7) lead to

$$p_3^+ = \frac{2(f_2 p_1^+ + f_1 p_2^+)}{(2 + 1/m_3) f_1 f_2 + (1 - m_1) f_2 \mathrm{e}^{-\mathrm{j}kl_1} + (1 - m_2) f_1 \mathrm{e}^{-\mathrm{j}kl_2}}, \tag{8}$$

where $f_1 = m_1 \cos kl_1 + \mathrm{j} \sin kl_1$, $f_2 = m_2 \cos kl_2 + \mathrm{j} \sin kl_2$, and $\mathrm{j} = \sqrt{-1}$ is the imaginary unit. The transmission loss of an anechoically terminated chamber is given by

$$TL = 10 \log_{10}(|p_1^+|^2 S_1 + |p_2^+|^2 S_2)/(|p_3^+|^2 S_3). \tag{9}$$

Substituting equation (8) into equation (9) yields

$$TL = 20 \log_{10}|(2 + 1/m_3) f_1 f_2 + (1 - m_1) f_2 \mathrm{e}^{-\mathrm{j}kl_1} + (1 - m_2) f_2 \mathrm{e}^{-\mathrm{j}kl_1}|$$
$$- 20 \log_{10} 2|f_1 + f_2(p_1^+/p_2^+)| + 10 \log_{10}(|p_1^+/p_2^+|^2 S_1 + S_2)/S_3. \tag{10}$$

Clearly, the transmission loss of the expansion chamber with two end-inlets and one side-outlet is a function of acoustic pressure ratio p_1^+/p_2^+ of the incident waves.

3. BOUNDARY ELEMENT APPROACH

The sound propagation in a duct is given by the well-known Helmholz equation as [13]

$$\nabla^2 P + k^2 P = 0, \tag{11}$$

where P is the acoustic pressure, $k = \omega/c$ is the wavenumber, ω is the angular frequency, and c is the sound speed. The boundary integral equation of this relationship can be represented as [14, 15]

$$C(X)P(X) = \int_\Gamma \left[G(X, Y) \frac{\partial P}{\partial n}(Y) - P(Y) \frac{\partial G}{\partial n}(X, Y) \right] \mathrm{d}\Gamma(Y). \tag{12}$$

Here Γ is the boundary surface of the acoustic domain, n is the unit outward normal vector on Γ, the function $G(X, Y) = \exp(-\mathrm{j}kR)/4\pi R$ is Green's function of free space, where $R = |X - Y|$ is the distance between any two points X and Y in the domain or on the surface, and $C(X)$ is a coefficient which depends on the position of point X.

A numerical solution of the boundary integral equation (12) can be achieved by discretizing the boundary surface of the domain into a number of elements. By using discretization and numerical integration, and introducing the momentum equation [13]

$$\mathrm{j}\rho\omega\bar{U} = -\nabla P, \tag{13}$$

the following algebraic system of equations is obtained:

$$[A]\{P\} = \rho c[B]\{U_n\}, \tag{14}$$

where $[A]$ and $[B]$ are the coefficient matrices, and $\{P\}$ and $\{U_n\}$ are the vectors whose elements are the sound pressure P and outward normal particle velocity U_n on the boundary nodes, respectively. The detailed treatment of the numerical solution procedure for the boundary element method in duct acoustics can be found elsewhere [15].

For the expansion chamber with two inlets and one outlet shown in Figure 1, the boundary surface can be divided into two inlets, outlet and wall, and then the variables in equation (14) are grouped as

$$[A_1 \;\; A_2 \;\; A_3 \;\; A_w] \begin{Bmatrix} P_1 \\ P_2 \\ P_3 \\ P_w \end{Bmatrix} = \rho c [B_1 \;\; B_2 \;\; B_3 \;\; B_w] \begin{Bmatrix} U_{n,1} \\ U_{n,2} \\ U_{n,3} \\ U_{n,w} \end{Bmatrix}, \tag{15}$$

where P_1, P_2, P_3 and P_w are vectors with dimensions N_1, N_2, N_3 and N_w, and subscripts 1, 2, 3 and w denote the corresponding quantities on the inlet 1, inlet 2,

outlet and wall respectively. For the rigid wall ($U_{n,w} = 0$), equation (15) may be rearranged as

$$\begin{Bmatrix} P_1 \\ P_2 \\ P_3 \\ P_w \end{Bmatrix} = \rho c [A_1 \;\; A_2 \;\; A_3 \;\; A_w]^{-1} [B_1 \;\; B_2 \;\; B_3] \begin{Bmatrix} U_1 \\ U_2 \\ U_3 \end{Bmatrix}, \tag{16}$$

where $\{U_1\} = -\{U_{n,1}\}$, $\{U_2\} = -\{U_{n,2}\}$, $\{U_3\} = \{U_{n,3}\}$, leading to

$$\begin{Bmatrix} P_1 \\ P_2 \\ P_3 \end{Bmatrix} = \rho c [T] \begin{Bmatrix} U_1 \\ U_2 \\ U_3 \end{Bmatrix}, \tag{17}$$

where $[T]$ corresponds to the first $N_1 + N_2 + N_3$ rows of $[A_1 \;\; A_2 \;\; A_3 \;\; A_w]^{-1}$ $[B_1 \;\; B_2 \;\; B_3]$. When the planar wave condition is satisfied at the inlets and outlet, $\{P_1\}$, $\{P_2\}$, $\{P_3\}$, $\{U_1\}$, $\{U_2\}$ and $\{U_3\}$ may be represented by p_1, p_2, p_3, u_1, u_2 and u_3, yielding

$$\begin{Bmatrix} p_1 \\ p_2 \\ p_3 \end{Bmatrix} = \rho c \begin{bmatrix} t_{11} & t_{12} & t_{13} \\ t_{21} & t_{22} & t_{23} \\ t_{31} & t_{32} & t_{33} \end{bmatrix} \begin{Bmatrix} u_1 \\ u_2 \\ u_3 \end{Bmatrix}, \tag{18}$$

where $t_{mn} = \sum T_{ij}/N_i$, and N_i is the dimension of $\{P_i\}$.

In terms of $p = p^+ + p^-$ and $\rho c u = p^+ - p^-$ for the plane wave propagation and $p_3^- = 0$ for the non-reflecting outlet, equation (18) may be written as

$$\begin{Bmatrix} p_1^- \\ p_2^- \\ p_3^+ \end{Bmatrix} = \begin{bmatrix} 1 + t_{11} & t_{12} & -t_{13} \\ t_{21} & 1 + t_{22} & -t_{23} \\ t_{31} & t_{32} & 1 - t_{33} \end{bmatrix} \begin{Bmatrix} (t_{11} - 1)p_1^+ + t_{12}p_2^+ \\ t_{21}p_1^+ + (t_{22} - 1)p_2^+ \\ t_{31}p_1^+ + t_{32}p_2^+ \end{Bmatrix}. \tag{19}$$

For a specified p_1^+/p_2^+, p_3^+/p_2^+ can be evaluated from equation (19) and then substituting into equation (9) to calculate the transmission loss of the present configuration.

4. RESULTS AND DISCUSSION

For all configurations, the present study considers $l = 54{\cdot}0$ cm and $d = 15{\cdot}32$ cm for the length and diameter of the chamber; $d_1 = d_2 = 4{\cdot}86$ cm and $d_3 = 5{\cdot}84$ cm for the inlet and outlet ducts. The chamber and two inlet ducts are concentric. The speed of sound in computations is 346 m/s.

To examine the effect of outlet location on the acoustic attenuation performance, Figures 2–5 present the transmission loss of the expansion chamber for four different outlet locations (Figure 2: $l_2 = l/8 = 6{\cdot}75$ cm, Figure 3: $l_2 = l/4 = 13{\cdot}5$ cm, Figure 4: $l_2 = 3l/8 = 20{\cdot}25$ cm, Figure 4: $l_2 = l/2 = 27{\cdot}0$ cm) with $p_1^+/p_2^+ = 1{\cdot}0$. Each figure compares the transmission loss from the boundary element predictions with the one-dimensional solutions. The BEM calculations are extended 10 cm into

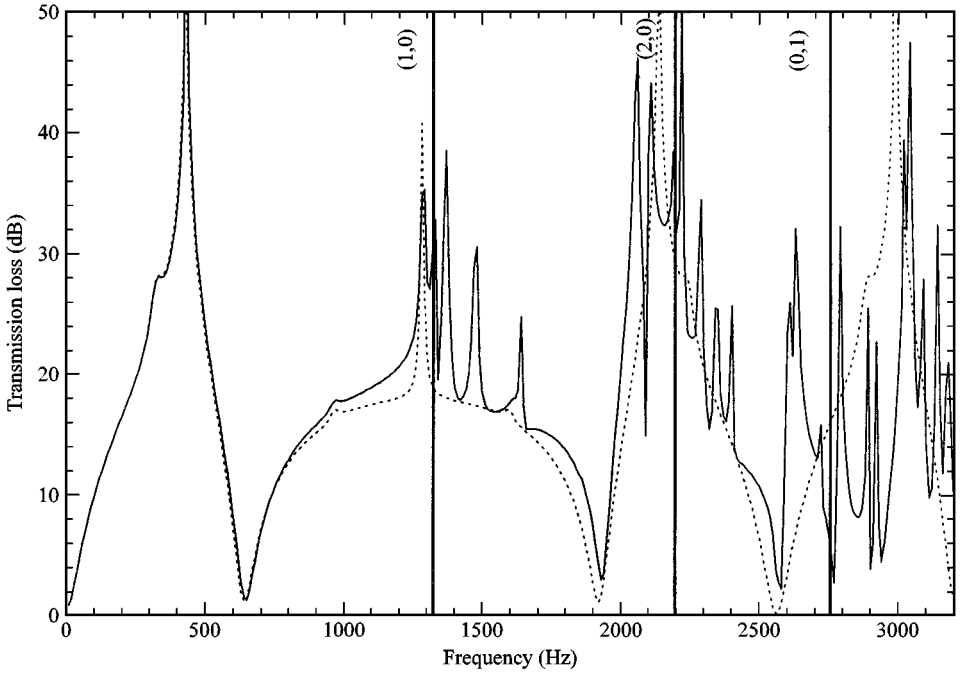

Figure 2. Transmission loss of expansion chamber with two end-inlets/one side-outlet ($d = 15{\cdot}32$ cm, $d_1 = d_2 = 4{\cdot}86$ cm, $d_3 = 5{\cdot}84$ cm, $l = 54{\cdot}0$ cm, $l_2 = 6{\cdot}75$ cm, $p_1^+/p_2^+ = 1{\cdot}0$): —, BEM; ·····, 1-D analytical.

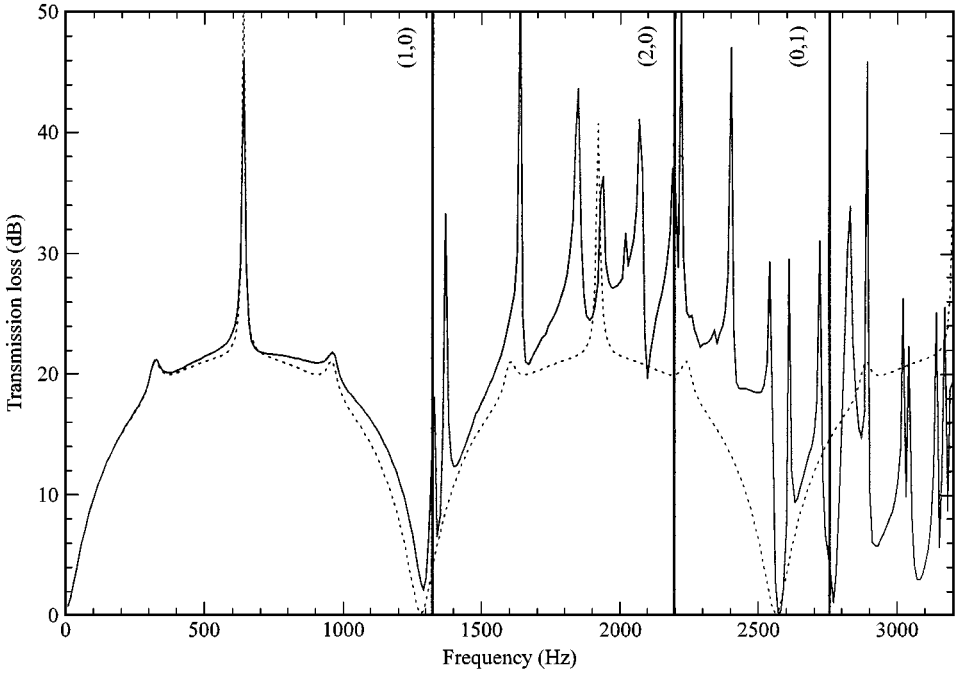

Figure 3. Transmission loss of expansion chamber with two end-inlets/one side-outlet ($d = 15{\cdot}32$ cm, $d_1 = d_2 = 4{\cdot}86$ cm, $d_3 = 5{\cdot}84$ cm, $l = 54{\cdot}0$ cm, $l_2 = 13{\cdot}50$ cm, $p_1^+/p_2^+ = 1{\cdot}0$): —, BEM; ·····, 1-D analytical.

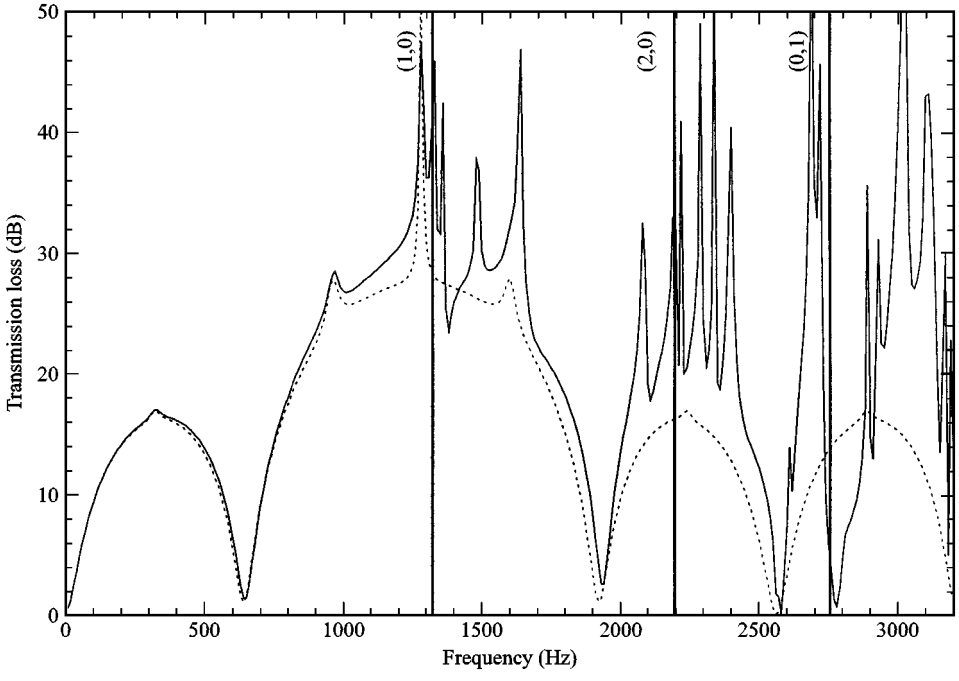

Figure 4. Transmission loss of expansion chamber with two end-inlets/one side-outlet ($d = 15{\cdot}32$ cm, $d_1 = d_2 = 4{\cdot}86$ cm, $d_3 = 5{\cdot}84$ cm, $l = 54{\cdot}0$ cm, $l_2 = 20{\cdot}25$ cm, $p_1^+/p_2^+ = 1{\cdot}0$): —, BEM; ·····, 1-D analytical.

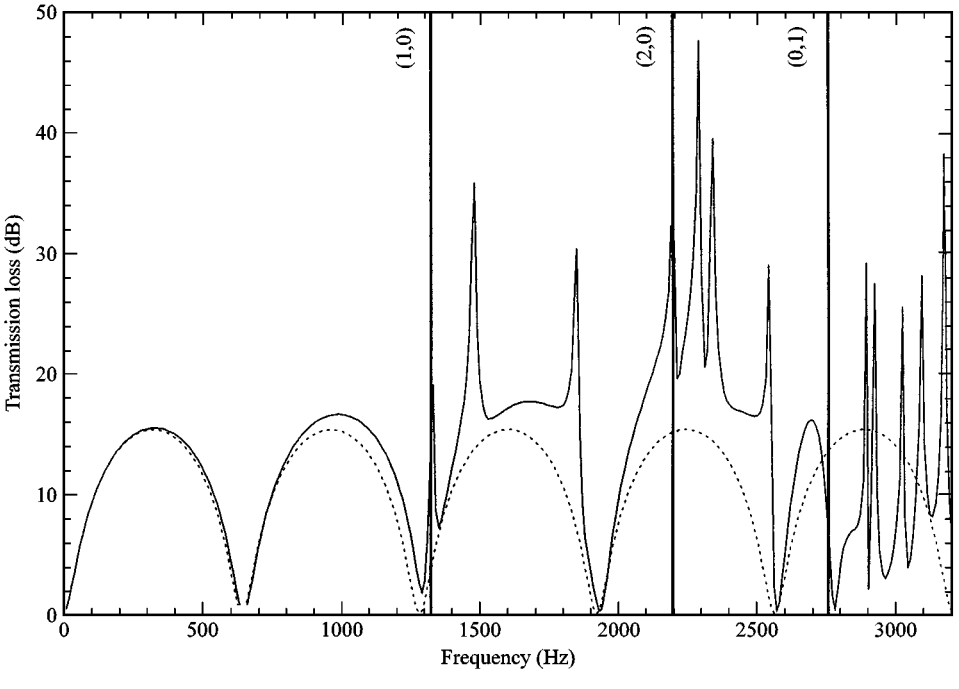

Figure 5. Transmission loss of expansion chamber with two end-inlets/one side-outlet ($d = 15{\cdot}32$ cm, $d_1 = d_2 = 4{\cdot}86$ cm, $d_3 = 5{\cdot}84$ cm, $l = 54{\cdot}0$ cm, $l_2 = 27{\cdot}0$ cm, $p_1^+/p_2^+ = 1{\cdot}0$): —, BEM; ·····, 1-D analytical.

inlet and outlet ducts so that the plane wave conditions at the inlets and outlet are satisfied. The one-dimensional solutions of transmission loss in Figures 2–5 show reasonable agreement with boundary element predictions at low frequencies, particularly below the first higher order mode (1,0) of the chamber. By ignoring the numerous sharp peaks in the boundary element results, the qualitative agreement appears to the reasonable until the (0,1) mode. With increasing frequency, multi-dimensional waves begin to dominate in the chambers, terminating the applicability of the 1-D approach. Thus, in applying the one-dimensional approach, the upper limit of frequency for a given configuration needs to be examined. The transmission loss in Figures 2–5 exhibits the superposition of the attenuation domes and the resonance peaks. It may be shown in 1-D approach that the resonance frequencies are dependent on the difference $l_1 - l_2$ and correspond to $l_1 - l_2 = (2n + 1)\lambda/2$, where $n = 0, 1, 2, \ldots$, and λ being the wavelength. As $l_1 - l_2$ is decreased, the resonance frequencies are increased.

The effect of incident wave condition on the acoustic attenuation of expansion chamber with two end-inlets and one side-outlet is illustrated by varying the acoustic pressure ratio p_1^+/p_2^+. Figures 6 and 7 depict the transmission loss results from the BEM and the 1-D approach for $p_1^+/p_2^+ = -1{\cdot}0$ and $p_1^+/p_2^+ = j$ with $l_2 = 6{\cdot}75$ cm. Compared to the in-phase incident waves $p_1^+/p_2^+ = 1{\cdot}0$ of Figure 2, Figures 6 and 7 reveal significantly different behaviour: The out-of-phase $p_1^+/p_2^+ = -1{\cdot}0$ of Figure 6 yields a desirable low-frequency attenuation (resonance),

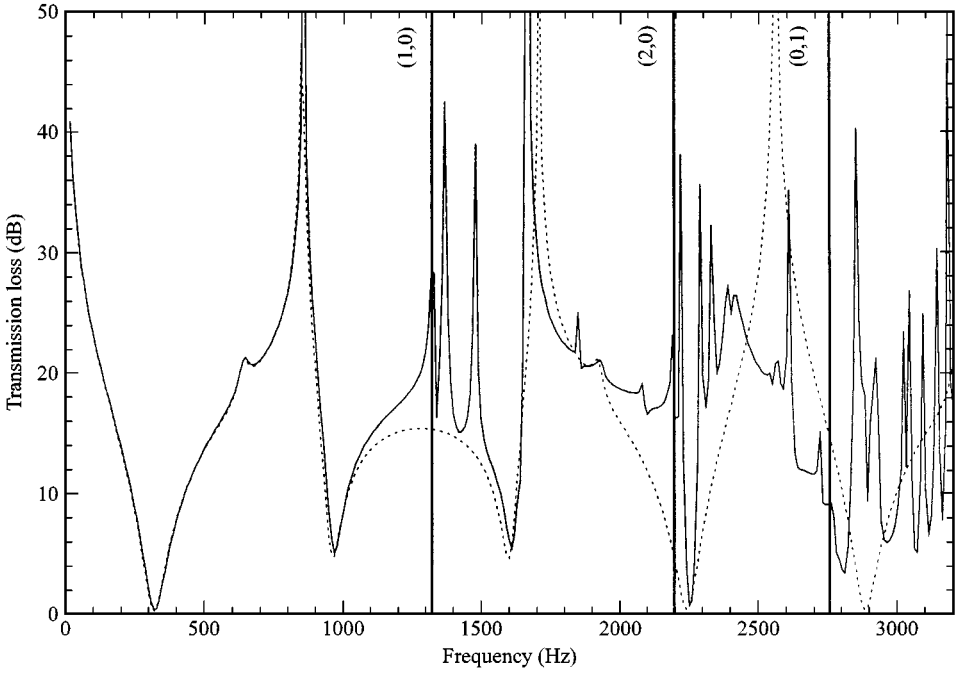

Figure 6. Transmission loss of expansion chamber with two end-inlets/one side-outlet ($d = 15{\cdot}32$ cm, $d_1 = d_2 = 4{\cdot}86$ cm, $d_3 = 5{\cdot}84$ cm, $l = 54{\cdot}0$ cm, $l_2 = 6{\cdot}75$ cm, $p_1^+/p_2^+ = -1{\cdot}0$): —, BEM; ·····, 1-D analytical.

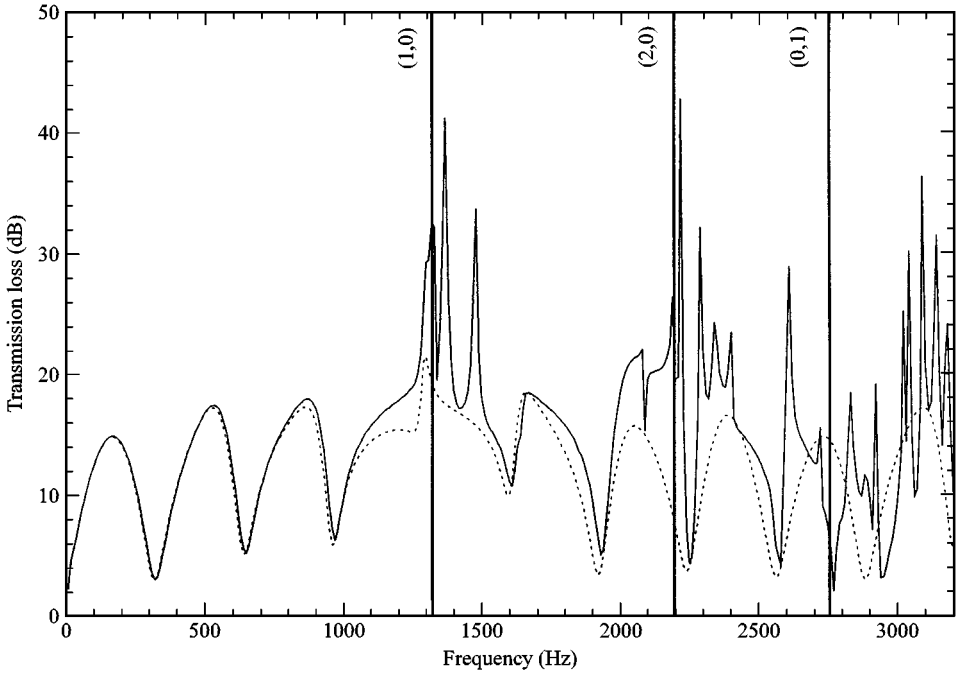

Figure 7. Transmission loss of expansion chamber with two end-inlets/one side-outlet ($d = 15{\cdot}32$ cm, $d_1 = d_2 = 4{\cdot}86$ cm, $d_3 = 5{\cdot}84$ cm, $l = 54{\cdot}0$ cm, $l_2 = 6{\cdot}75$ cm, $p_1^+/p_2^+ = j$): —, BEM; ·····, 1-D analytical.

while the 90° phase angle $p_1^+/p_2^+ = j$ of Figure 7 changes the transmission loss considerably and moves the first resonance to higher frequencies. As expected, Figures 6 and 7 again exhibit a resonable agreement between the 1-D solutions and boundary element predictions until the (1,0) mode, and a qualitative agreement until the (0,1) mode when numerous sharp peaks are ignored.

To conclude, the present study (1) provides a simple 1-D solution for the acoustic attenuation of an expansion chamber with two end-inlets and one side-outlet; (2) compares the 3-D boundary element predictions and the 1-D analytical results to assess the accuracy and applicability of the latter; (3) demonstrates the effect of outlet location; and (4) illustrates the importance of relative phase information of two incident waves at the inlets.

REFERENCES

1. A. I. El-Sharkawy and A. H. Nayfeh 1978 *Journal of the Acoustical Society of America* **63**, 667–674. Effect of the expansion chamber on the propagation of sound in circular pipes.
2. L. J. Erikkson 1980 *Journal of the Acoustical Society of America* **68**, 545–550. Higher order mode effects in the circular ducts and expansion chambers.
3. L. J. Eriksson 1982 *Journal of the Acoustical Society of America* **72**, 1208–1211. Effect of inlet/outlet locations on higher order modes in silencers.
4. J. G. Ih and B. H. Lee 1985 *Journal of the Acoustical Society of America* **77**, 1377–1388. Analysis of higher-order mode effects in the circular expansion chamber with mean flow.

5. J. KIM and W. SOEDEL 1989 *Journal of Sound and Vibration* **129**, 237–254. General formulation of four pole parameters for three-dimensional cavities utilizing modal expansion, with special attention to the annular cylinder.
6. A. D. SAHASRABUDHE, S. A. RAMU and M. L. MUNJAL 1991 *Journal of Sound and Vibration* **147**, 371–394. Matrix condensation and transfer matrix techniques in the 3-D analysis of expansion chamber mufflers.
7. A. SELAMET and P. M. RADAVICH 1997 *Journal of Sound and Vibration* **201**, 407–426. The effect of length on the acoustic attenuation performance of concentric expansion chambers: an analytical, computational, and experimental investigation.
8. A. SELAMET and Z. L. JI 1998 *Journal of Sound and Vibration* **213**, 601–617. Acoustic attenuation performance of circular expansion chambers with offset inlet/outlet: I. Analytical approach.
9. A. SELAMET, Z. L. JI and P. M. RADAVICH 1998 *Journal of Sound and Vibration* **213**, 619–641. Acoustic attenuation performance of circular expansion chambers with offset inlet/outlet: II. Comparison with experimental and computational studies.
10. S. I. YI and B. H. LEE 1986 *Journal of the Acoustical Society of America* **79**, 1299–1306. Three-dimensional acoustic analysis of a circular expansion chamber with a side inlet and a side outlet.
11. S. I. YI and B. H. LEE 1987 *Journal of the Acoustical Society of America* **81**, 1279–1287. Three-dimensional acoustic analysis of circular expansion chambers with side inlet and end outlet.
12. M. L. MUNJAL 1997 Applied Acoustics **52**, 165–175. Plane wave analysis of side inlet/outlet chamber mufflers with mean flow.
13. M. L. MUNJAL 1987 *Acoustics of Ducts and Mufflers*. New York: Wiley–Interscience.
14. A. F. SEYBERT and C. Y. R. CHENG 1987 *Journal of Vibration, Acoustics, Stress, and Reliability in Design* **109**, 15–21. Application of the boundary element method to acoustic cavity response and muffler analysis.
15. Z. L. JI, Q. MA and Z. H. ZHANG 1994 *Journal of Sound and Vibration* **173**, 57–71. Application of the boundary element method to predicting acoustic performance of expansion chamber mufflers with mean flow.